Design and Implementation of Color-Shift Keying for Visible Light Communications

Eric Monteiro, *Member, IEEE*, and Steve Hranilovic, *Senior Member, IEEE*

***Abstract*—Color-shift keying (CSK) is a visible light communication intensity modulation scheme, outlined in IEEE 802.15.7, that transmits data imperceptibly through the variation of the color emitted by red, green, and blue light emitting diodes. An advantage of CSK is that the power envelope of the transmitted signal is fixed; therefore, CSK reduces the potential for human health complications related to fluctuations in light intensity. In this work, a rigorous design framework for high order CSK constellations is presented. A key benefit of the frame work is that it optimizes constellations while accounting for crosstalk between the color communication channels. In addition, and unlike previous approaches, the method is capable of optimizing 3-D constellations. Furthermore, a prototype CSK communication system is presented to validate the performance of the optimized constellations, which provide gains of 1–3 dB over standard 805.15.7 constellations.**

***Index Terms*—Color-shift keying (CSK), intensity modulation, visible light communications (VLC).**

I. Introduction

THE use of indoor solid-state light-emitting diode (LED) luminaries for a dual communications role has recently received attention as a potential means to reduce the spectral load on radio cell systems. The emissions from these visible light communication (VLC) systems cannot penetrate opaque surfaces and are envisioned to offload mobile data without interfering with radio frequency (RF) transceivers. These VLC systems send data by modulating the instantaneous intensity of a luminary rapidly enough so as not to be perceivable. Luminaries equipped with red-green-blue (RGB) LEDs can also modify the perceived color of illumination, as seen in recent commercial products [1]. However, there are currently few rigorous frameworks concerning the optimization of multicolored LED modulation formats.

Three VLC specific modulation formats designed for RGB LEDs have been discussed in the literature: color intensity modulation (CIM), color-shift keying (CSK), and metameric modulation (MM). In CIM, data are encoded onto the instantaneous intensity of an LED luminary while maintaining a static perceived color [2]. Although this framework is general, only initial steps in the design of constellations have been performed. In [2] constellation design for CIM is considered through the maximization of mutual information for a desired perceived static color. However, the designs were achieved through a time consuming exhaustive search in place of an optimization algorithm. CSK is a more constrained version of CIM where the signal envelope has a non-varying power [3]. The advantage of CSK is that intensity fluctuations, as observed by the human eye, are less than those of CIM. Therefore, CSK limits the potential for human health complications, such as nausea or epilepsy, related to fluctuations in light intensity [4]. In the case of CSK, the IEEE 802.15.7 standard provides 4, 8 and 16 point CSK constellations for communications at rates of up to 96 Mbps. In [5], CSK constellations are optimized against potential crosstalk using a statistical sphere packing technique; however, the link between the optimized constellations and perceived color is not provided. In [6], CSK constellations are optimized by minimizing the symbol error rate (SER) via non uniform signaling. However, this work enumerates the constraint region in place of optimization, and only demonstrates binary constellations that do not consider crosstalk between the three color channels. MM further constrains CSK by requiring that all emitted symbols have a fixed instantaneous perceived output color [7]. MM has the same advantage as CSK, with the additional benefit of greater control over the color quality of the luminary. However, the disadvantage of MM is that it requires the use of a secondary, independently controlled, green LED [7].

In this work, a rigorous framework for the design of CSK symbol sets, based on deterministic optimization, is presented [8]. This framework allows constellations of an arbitrary size to be designed and, unlike previous optimization attempts, simultaneously accounts for potential crosstalk between the color channels (Section II) and the study of colorimetry (Section III-B) such that the source color may be adjusted to meet lighting industry illumination standards. Additionally, the framework is uniquely adapted to produce 3-D CSK constellations that allow for a specified ripple in the output intensity of the luminary. This paper concludes with details on a CSK prototype to verify channel model assumptions and to compare the performance of constellations optimized for the prototype channel against the performance of constellations designed using the IEEE 802.15.7 design rules.

II. CSK Channel Model

Fig. 1 depicts a block diagram of a CSK communication system. In this work, CSK symbols are represented by the

Manuscript received November 12, 2013; revised February 13, 2014 and March 26, 2014; accepted March 26, 2014. Date of publication March 27, 2014; date of current version May 12, 2014. This work was supported by the Natural Sciences and Engineering Research Council of Canada through Discovery and Strategic Projects Grants. This paper was presented in part at the 2012 IEEE Workshop on Optical Wireless Communications and at IEEE Globecom 2012.

The authors are with the Department of Electrical and Computer Engineering, McMaster University, Hamilton, ON L8S 4K1, Canada (e-mail: monteie@mcmaster.ca; hranilovic@mcmaster.ca).

Color versions of one or more of the figures in this paper are available online at http://ieeexplore.ieee.org.

Digital Object Identifier 10.1109/JLT.2014.2314358

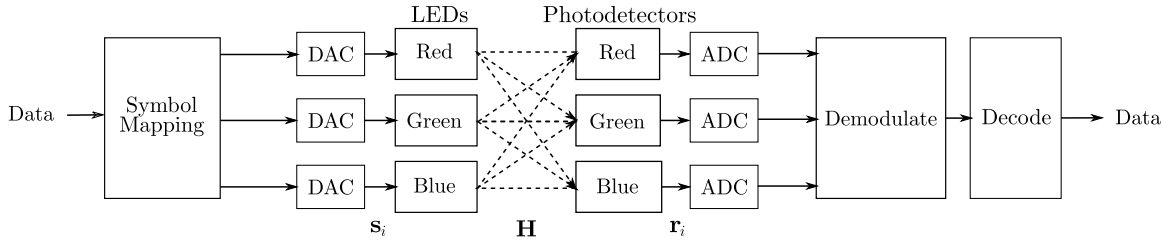

Fig. 1. Functional block diagram of the VLC channel that supports the CSK modulation format.

instantaneous current driving each RGB LED. An N point CSK constellation is defined as the collection of triplets

$$\mathcal{A} = \{\mathbf{s}_1, \mathbf{s}_2, \mathbf{s}_3, \ldots, \mathbf{s}_N\} \tag{1}$$

where

$$\mathbf{s}_j = [\, i_{\mathrm{r},j} \quad i_{\mathrm{g},j} \quad i_{\mathrm{b},j} \,] \tag{2}$$

with $i_{\mathrm{r},j}$, $i_{\mathrm{g},j}$, and $i_{\mathrm{b},j}$ [A] representing the average current in each of the red, green, and blue colored LEDs respectively for the jth symbol.

Following electrical-to-optical conversion, the optical signal propagates through free space and is detected by a set of three filtered photodetectors to produce output photocurrents. The CSK channel is thus three coupled intensity modulated direct detection channels related by the channel gain matrix

$$\mathbf{H} = \begin{bmatrix} h_{\mathrm{r,r}} & h_{\mathrm{r,g}} & h_{\mathrm{r,b}} \\ h_{\mathrm{g,r}} & h_{\mathrm{g,g}} & h_{\mathrm{g,b}} \\ h_{\mathrm{b,r}} & h_{\mathrm{b,g}} & h_{\mathrm{b,b}} \end{bmatrix}$$

where $h_{j,k}$ represents the channel gain between the electrical current input and the received photocurrents from transmitter k to receiver j. In practice, the elements of $\mathbf{H}$ vary with LED drive current due to the non-linear relationship between the optical power and electrical current of an LED [9]. However, to make the problem of optimizing constellations more tractable, $\mathbf{H}$ is assumed to be static over all drive currents. In addition, the channel is assumed flat (no inter-symbol interference) with $\mathbf{H}$ being measurable and invertible. Assuming a rectangular pulse shape and additive white Gaussian noise (AWGN), the equivalent discrete time baseband channel model is given by

$$\mathbf{r}_i = \mathbf{H}\mathbf{s}_i + \mathbf{n}_i \tag{3}$$

where $\mathbf{r}_i$ is the received symbol and $\mathbf{n}_i$ is the AWGN noise vector [10].

III. CSK Constellation Optimization

A. Intensity Constraint Formulation

As perceivable fluctuations in light intensity have known human health risks, the IEEE 802.15.7 standard for CSK attempts to minimize the potential for intensity fluctuations by constraining the total optical power (luminous flux) of each symbol to be equal [3]. Let η_{r}, η_{g}, and η_{b} denote the optical gain of each LED in units of lumens per ampere [lm/A] with

$$\overline{\eta} = [\, \eta_{\mathrm{r}} \quad \eta_{\mathrm{g}} \quad \eta_{\mathrm{b}} \,].$$

The instantaneous luminous flux (optical power) of the jth symbol is

$$\mathcal{L}(\mathbf{s}_j) = \langle \overline{\eta}, \mathbf{s}_j \rangle$$

where $\langle \cdot \rangle$ is the inner product. The IEEE 802.15.7 standard thus requires

$$\forall i \quad \mathcal{L}(\mathbf{s}_i) = L$$

for some fixed average luminous flux L.

Since typical CSK modems are envisioned to operate at signaling rates in excess of 1 MHz, the impact of flicker (in luminous flux or color) on human health is negligible, which suggests that some variation in the power envelope of CSK symbols is acceptable [4]. Therefore, in general,

$$L_{\min} \leq \mathcal{L}(\mathbf{s}_i) \leq L_{\max} \tag{4}$$

where $L_{\min}$ and $L_{\max}$ are the minimum and maximum allowable total luminous flux respectively. Constant luminous flux signaling is achieved when $L_{\min} = L_{\max}$. Furthermore, non-negativity and peak current constraints on each LED require that

$$\mathbf{0} \preceq \mathbf{s}_i \preceq [\, I_{\mathrm{r}} \quad I_{\mathrm{g}} \quad I_{\mathrm{b}} \,] \tag{5}$$

where I_r, I_g, and I_b are the peak current of the red, green and blue LEDs respectively. Note that this formulation can be generalized to apply to CIM by setting $L_{\min} = 0$ and $L_{\max} = \infty$ such that only the peak current constraints are active.

A convenient aspect of this formulation is that it is easily adapted to design constellations of constant current in place of constant luminous flux. Define

$$\mathcal{I}(\mathbf{s}_j) = i_{\mathrm{r},j} + i_{\mathrm{g},j} + i_{\mathrm{b},j}$$

as the total instantaneous current of symbol j. Let $I_{\min}$ and $I_{\max}$ represent the minimum and maximum allowable total LED drive current. Then, by replacing (4) with

$$I_{\min} \leq \mathcal{I}(\mathbf{s}_i) \leq I_{\max} \tag{6}$$

the total electrical current of the system becomes constrained in place of the total optical power. Therefore, this formulation provides the designer with the freedom to either fix the optical power to limit potential flicker, or to fix the electrical current to limit the potential for RF radiation caused by high current switching through stray inductance [11].

Note that in practice η_{r}, η_{g}, and η_{b} decay, at different rates, with device age. These changes in $\overline{\eta}$ are represented by changes in $\mathbf{H}$ which can cause the color of the luminary to drift over time. Therefore, CSK systems require additional circuitry to

compensate for this drift. Additionally, this implies that a constellation optimized for a specific $\mathbf{H}$ becomes less effective over the lifetime of the luminary.

B. Color Constraint Formulation

IEEE 802.15.7 also adheres to all applicable luminary standards (e.g., [12]), which restrict the color output of a luminary. The most widely used model of human color perception is the CIE 1931 *chromaticity* gamut [13]. The color of any visible light spectral power density (SPD) can be represented by the chromaticity coordinates $[x, y]$.

Suppose that, given a set of RGB LEDs, a desired output chromaticity of $[x_\mathrm{d}, y_\mathrm{d}]$ is required. Let $[x_\mathrm{r}, y_\mathrm{r}]$, $[x_\mathrm{g}, y_\mathrm{g}]$, and $[x_\mathrm{b}, y_\mathrm{b}]$ represent the chromaticity coordinates of the red, green, and blue LEDs respectively. The relative luminous flux between the RGB LEDs, denoted by $\mathbf{d}$, required to produce the desired chromaticity can be derived from

$$\begin{bmatrix} \frac{x_\mathrm{r}}{y_\mathrm{r}} & \frac{x_\mathrm{g}}{y_\mathrm{g}} & \frac{x_\mathrm{b}}{y_\mathrm{b}} \\ 1 & 1 & 1 \\ \frac{1-x_\mathrm{r}-y_\mathrm{r}}{y_\mathrm{r}} & \frac{1-x_\mathrm{g}-y_\mathrm{g}}{y_\mathrm{g}} & \frac{1-x_\mathrm{b}-y_\mathrm{b}}{y_\mathrm{b}} \end{bmatrix} \mathbf{d} = \begin{bmatrix} \frac{x_\mathrm{d}}{y_\mathrm{d}} \\ 1 \\ \frac{1-x_\mathrm{d}-y_\mathrm{d}}{y_\mathrm{d}} \end{bmatrix}. \tag{7}$$

Notice that the elements of $\mathbf{d}$ sum to one by definition. The constraint on the perceived chromaticity of a luminary can then be expressed by

$$\frac{1}{N}\sum \mathcal{L}(\mathbf{s}_j) = L\mathbf{d}. \tag{8}$$

If $L_\mathrm{min} < L_\mathrm{max}$, the value of L may be specified as part of the design or be treated as a design variable. Note that (8) implicitly assumes that the SPD of an LED scales linearly over the allowable range of driving currents; i.e., LED color is not a function of intensity (L).

C. Objective

For the AWGN model in (3), at high signal-to-noise ratios (SNRs) and with uniform signaling, the SER is dominated by the the minimum pairwise Euclidean distance between all received symbols in the alphabet. In the case of bounded luminous flux, the symbol set $\{\mathbf{s}_i\}$ that maximizes the minimum distance for a given SNR is given by

$$\begin{aligned} \mathcal{A} = \arg\max_{\{\mathbf{s}_i\}} \quad & \min_{j\neq k} \|\mathbf{H}(\mathbf{s}_j - \mathbf{s}_k)\|_2 \\ \text{s.t.} \quad & L_\mathrm{min} \leq \mathcal{L}(\mathbf{s}_i) \leq L_\mathrm{max} \\ & \mathbf{0} \preceq \mathbf{s}_j \preceq [\, I_\mathrm{r} \quad I_\mathrm{g} \quad I_\mathrm{b} \,] \\ & \tfrac{1}{N}\textstyle\sum \mathcal{L}(\mathbf{s}_i) = L\mathbf{d}. \end{aligned} \tag{9}$$

For bounded current, the first constraint is replaced by (6).

Notice that, unlike the constraints, the objective is both non-convex and non-differentiable making it incompatible with efficient, gradient based numerical optimization tools. For non-convex problems, optimization algorithms are only capable of recognizing local minima. Furthermore, the minima obtained by any algorithm depend on the initial estimate of the constellation used to start the optimization process. However, as the global optimal solution is non-unique, the likelihood of discovering a global optima is improved by optimizing the objective multiple times over a small set of random starting points. In order to overcome the non-differentiability of (9), a continuous approximation to the minimum function

$$\min_i\{d_i\} \simeq -\ln\left(\sum_i \exp(-\beta d_i)\right) \Big/ \beta \tag{10}$$

is used, where $\{d_i\}$ is the set of pairwise distances and β is a large positive scalar that determines the accuracy of the approximation [14]. Provided that one of the d_i is sufficiently small compared to the others, this function returns an approximation to the smallest d_i. Applying (10) to (9), the objective becomes

$$\arg\max_{\{\mathbf{s}_j\}} -\ln\left(\sum_{j\neq k} \exp(-\beta\|\mathbf{H}(\mathbf{s}_j - \mathbf{s}_k)\|_2)\right) \Big/ \beta \tag{11}$$

subject to the constraints in (9).

TABLE I
NUMERICAL OPTIMIZATION ALGORITHM

$\{\mathbf{s}_j\} \leftarrow$ random set of starting points
$\beta \leftarrow 1$
while $\beta < \beta_\mathrm{stop}$ **do**
  $\mathcal{A} \leftarrow$
    $\arg\max -\ln(\sum_{j\neq k} \exp(-\beta\|\mathbf{H}(\mathbf{s}_j - \mathbf{s}_k)\|_2))/\beta$
  $\beta \leftarrow 2\beta$
  $\{\mathbf{s}_j\} \leftarrow \mathcal{A}$
end while

D. Numerical Optimization

While (11) is readily solvable with any optimization toolkit, the smallest enumerated distances between all symbols approach the same value when near a local optima. This implies that for a given β, the approximation of the minimum in (10) becomes less reliable near a local minima. This issue can be alleviated by setting β to a fixed large value, however, this results in large gradients leading to numeric instability and convergence problems. A reasonable approach to obtain a reliable approximation without poor convergence is to progressively increase the value of β in a series of sequential optimization problems; summarized in Table I. The process of doubling β continues until the mean squared error between the constellations in the current and past iterations is less than a specified threshold. The optimization of the objective at each value of β is carried out using the interior point method of the *fmincon* function provided in the MATLAB optimization toolkit [15]. The fmincon function stops when the first order optimality measure, defined as the maximum of the stationarity and complementary slackness Karush–Kuhn–Tucker conditions, is less than a specified tolerance.

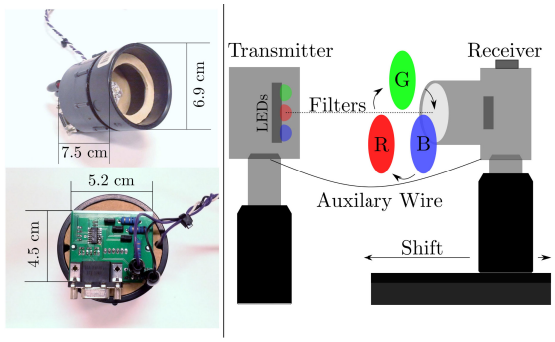

Fig. 2. CSK experimental test bed and photographs of the implemented transmitter.

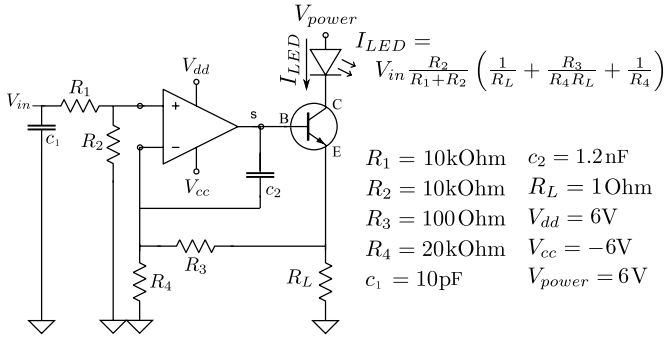

Fig. 3. Linear variable current driver.

IV. CSK Prototype

Fig. 2 shows a diagram of the experimental test bed used for measuring the error performance of CSK constellations. The transmitter is mounted on a optical post with the center of the luminary aligned with the center of the receiver aperture. The receiver is mounted on a rail nominally 1 m from the transmitter. Additionally, an auxiliary wire between the transmitter and receiver is used for synchronization purposes. All three color bands are transmitted simultaneously while the single element receiver independently captures each color channel in turn by cycling between the red, green, and blue filters.

A. Transmitter

The transmitter consists of an FPGA for data modulation [16], a 10-bit three channel video graphic array (VGA) digital-to-analog converter (DAC) [17], three custom high power linear current drivers [18], [19], and three colored LEDs [9]. Both the VGA DAC and FPGA are standard components on the Terasic DE2-70 Altera FPGA development board. The circuit shown in Fig. 3 is the variable current driver designed for this work. The resistor, R_L, acts as a current sensor for the amount of current being sunk into the LED. The voltage across R_L feeds back into the negative input of the OP AMP such that if a potential, v, is applied to the non inverting input of the device, the OP AMP will increase or decrease its output voltage until the current through R_L is equal to v/R_L, provided $R_4 \gg R_3$. The open collector nature of the driver allows the driver to linearly sink 0 to 1 A with the high voltage headroom, typically 3 V per

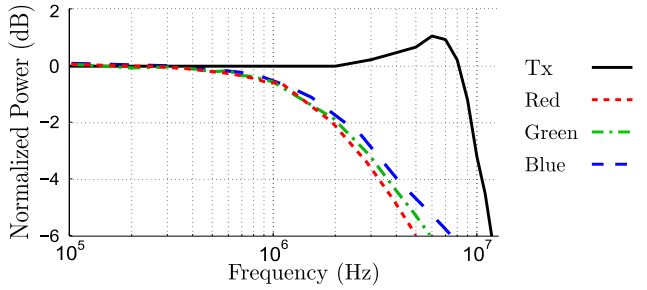

Fig. 4. Normalized power gain (dB) versus frequency (Hz) of a 200 mA peak to peak drive current, for the CSK channel at the input of the LED string (Tx) and output amplified photo-diode (Red, Green, Blue).

LED, required by the illumination LEDs in the output string. However, due to the non-linear relationship between the drive current and the emitted light power of LEDs, the first 8 bits of the DAC are assigned to drive each LED up to a 200 mA limit. The remaining 2 bits are not used in this work and are reserved to allow the driver to exceed the 200 mA current limit for future applications, such as linearizing the LED output power.

B. Receiver

The receiver consists of a single unity gain, 10 MHz bandwidth, photodiode [20], a one inch focal length bi-convex imaging optical concentrator, a set of colored polyester optical filters [21], a digital sampling oscilloscope (DSO) [22], and MATLAB scripts for post measurement digital signal processing [15]. The optical clock for all experimental measurements is limited to 100 kHz in order to allow the channel to appear flat without the use of equalization. The DSO was configured to operate with a sampling rate of 2.5 MSa/s oversampling the data with 25 samples per symbol. Oversampling allows a matched filter to be implemented in MATLAB. As rectangular pulses are received, the matched filter is the average of received symbol samples. Furthermore, the SNR of the received signal can be adjusted by varying the number of samples averaged per symbol (up to 25), allowing for efficient measurement of the SER versus SNR of the experimental channel. Let N_s denote the number of samples to average. The SNR after matched filtering is

$$\text{SNR} = \frac{m^2 N_s}{\sigma^2} \tag{12}$$

where σ^2 is the variance of the noise process before matched filtering, and m represents the sum of the received RGB channel means. Notice that in the case of an AWGN channel, this process is equivalent to either scaling the transmitted optical power through duty cycling or varying the data rate. Synchronization is guaranteed as the symbol clock from the transmitter is directly sampled by the receiver. Following the matched filter, decoding, detailed in Section VI, is performed.

C. Channel Characterization

1) Bandwidth: Fig. 4 shows the measured normalized power gain versus frequency from the input of the driver to emitter of the bipolar junction transistor (Tx) and from the input of the

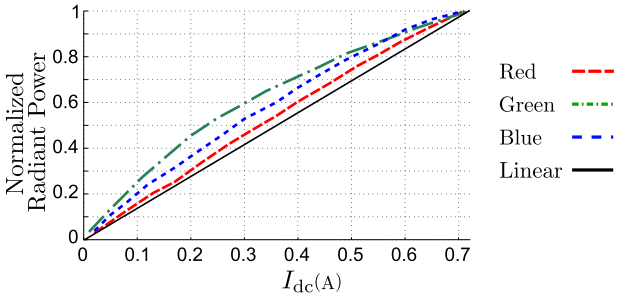

Fig. 5. Normalized received power versus LED drive current.

driver to the output of the photodetector for each color channel. It can be seen that the 3 dB bandwidth of each color channel is approximately 3 MHz, limited by the modulation bandwidth of the LEDs.

2) Noise: The noise was characterized on each channel while the source was off (ambient light only) and while each source was on (powered with 200 mA direct current). For both the on and off cases, the noise samples passed the chi-squared test for Gaussianity at the 5% significance level. Furthermore, there was a difference of less than 0.1 dB in noise power between the on and off cases. Therefore, the receiver noise is well-modelled as signal-independent and dominated by thermal noise and ambient light induced shot noise. In measurements, the noise has a nominal variance of 1.42×10^{-6} [A^2] for each channel. As the measurement for the red, green and blue channels are performed at different times with the same detector under the same test conditions, the noise statistics for each of color bands are identical. These observations suggest that the signal-independent AWGN assumption for the VLC channel in (3) is reasonable.

3) Linearity: Fig. 5 depicts the normalized photo-response of each color channel versus LED DC drive current, denoted by $I_{\rm dc}$, and compares them to the ideal linear channel response. The DC transfer characteristics of the red, green, and blue channels can be modeled by the third order polynomials

$$\begin{aligned} r_{\rm dc} &= -0.3854 I_{\rm dc}^3 + 0.1423 I_{\rm dc}^2 + 1.3828 I_{\rm dc} \\ g_{\rm dc} &= 1.526 I_{\rm dc}^3 - 2.8723 I_{\rm dc}^2 + 2.5712 I_{\rm dc} \\ b_{\rm dc} &= 0.2096 I_{\rm dc}^3 - 0.8201 I_{\rm dc}^2 + 1.7719 I_{\rm dc} \end{aligned} \tag{13}$$

where $r_{\rm dc}$, $g_{\rm dc}$, $b_{\rm dc}$ are the normalized optical power of red, green, and blue channels respectively. It is clear from Fig. 5 that each channel, particularly the green channel, is significantly non-linear over the LEDs input current range. Hence, the experimental current limit is set to 200 mA to mitigate non-linear channel effects.

D. Channel Estimation

Channel estimation is carried out by applying a known DC current to each channel independently, and then recording the photo-response of each detector to each LED. The choice of the DC current for channel estimation has an impact on the measured channel matrix. For a 200 mA test current, the channel matrix is given by

$$\mathbf{H}_{200} = 55.3 \times 10^{-3} \begin{bmatrix} 1 & 0.042 & 0.030 \\ 0.194 & 0.665 & 0.277 \\ 0.009 & 0.084 & 0.421 \end{bmatrix} \tag{14}$$

while for a 100 mA current, the channel matrix becomes

$$\mathbf{H}_{100} = 56.4 \times 10^{-3} \begin{bmatrix} 1 & 0.030 & 0.024 \\ 0.195 & 0.623 & 0.258 \\ 0.008 & 0.077 & 0.414 \end{bmatrix}. \tag{15}$$

In both cases the channel matrix is full rank guaranteeing a unique mapping between the transmitter and receiver signal spaces. However, it is evident that the non-linear transfer characteristics of the LEDs impact the channel measurement, and that each CSK symbol will experience a unique channel matrix.

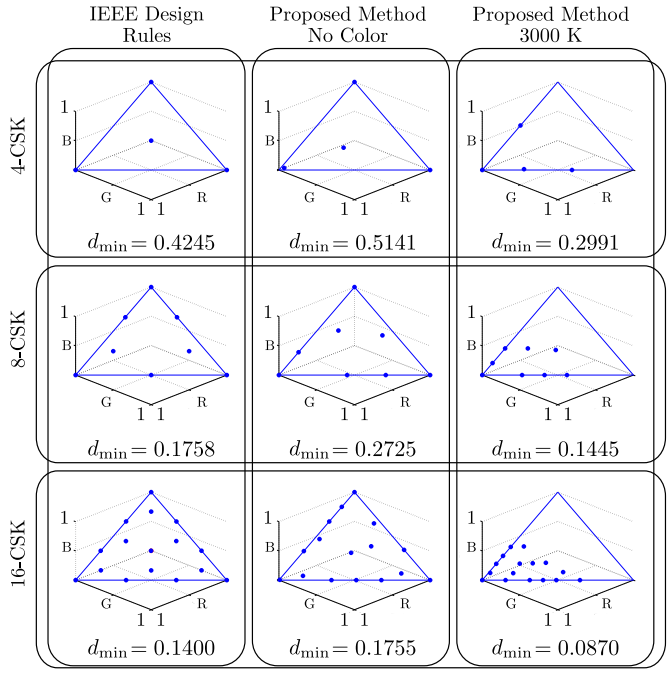

Fig. 6. CSK constellations designed for the prototype CSK channel using the IEEE design rules, and the proposed optimization technique with and without a specified operating chromaticity.

V. Optimized CSK Constellations

As flicker is not noticeable at high data rates, the constellations designed in this section assume constant current in place of constant luminous flux. In this case (6) replaces (4) in (9) and $I_{\min} = I_{\max}$. Fig. 6 depicts nine constant current CSK constellations, $\{\mathbf{s}_j\}$, designed for the prototype CSK channel discussed in Section IV assuming that the channel is nominally represented by $\mathbf{H}_{100}$ [1]. The quantity $d_{\min}$ represents the minimum Euclidean distance between the points in the set $\{\mathbf{H}_{100}\mathbf{s}_j\}$. Each dot represents a symbol, $\mathbf{s}_j$, sent by the transmitter and the plotted lines represent the plane of a one ampere constant current.

[1]The numeric values of each designed constellation can be found in the Appendixes of [23].

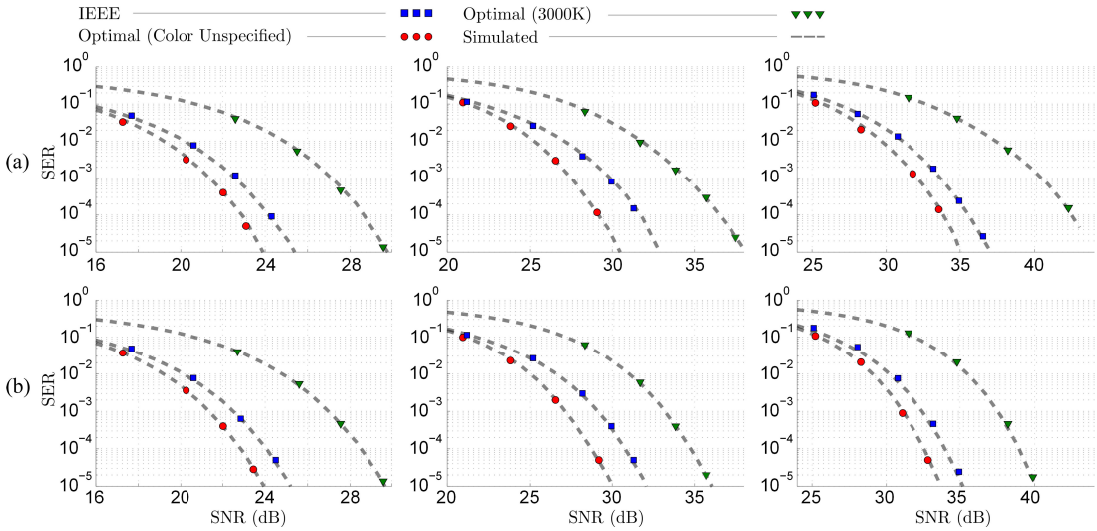

Fig. 7. Experimental SER versus electrical SNR for 4, 8 and 16-CSK. (a) Fixed Decoder (b) Optimal Decoder.

Three different design rules are employed. In the first column, constellations were designed using the IEEE 802.15.7 design rules [3, Sec. XII.2]. In the second column, the design method in Section III-D is used with the channel represented by $\mathbf{H}_{100}$, and without a chromaticity constraint. In the last column, the design method in Section III-D is repeated for a 3000K luminary common in household lighting [12]. A 3000K luminary has a desired chromaticity of $[x_{\mathrm{d}}, y_{\mathrm{d}}] = [0.4362, 0.4061]$, with $\mathbf{d} = [\,0.3755 \quad 0.5988 \quad 0.0256\,]$ for the RGB LEDs in [9].

For each optimized constellation, the best local minima over forty starting points selected from a uniform probability distribution is reported. An important observation is that the optimized constellations (Fig. 6, Col. 2) have a 1.68 dB, 3.81 dB and 1.96 dB gain in minimum distance for 4, 8 and 16-CSK respectively, when compared to the IEEE 802.15.7 standard constellations (Fig. 6, Col. 1). However, optimizing for a 3000K luminary (Fig. 6, Col. 3) caused a significant penalty in minimum distance, corresponding to a 4.70 dB, 5.51 dB, and 6.10 dB loss for the 4, 8, and 16-CSK constellations respectively when compared to the optimal case under no color constraints (Fig. 6, Col. 2). While the constellations without a chromaticity constraint (Fig. 6, Col. 1 & 2) have greater minimum distance than the 3000K luminaries, the average SPD produced by these constellations lie outside lighting industry standards (e.g., [12]). The penalty in $d_{\min}$ is a result of the desired chromaticity being far from the centroid of the constraint region. Notice that the third element (blue) of $\mathbf{d}$ is an order of magnitude less than the red and green channels; therefore, the power of the blue channel is restricted in order to meet the color requirements. As a result, the degrees of freedom available to the optimization algorithm, while meeting the desired chromaticity, are reduced.

VI. Experimental Results

All devices and measurement equipment were powered up and left idle for 30 min to allow them to settle into a nominal operating temperature state. Data were sampled as discussed in Section IV with the information decoded, in MATLAB, using two different decoding schemes.

While the constellations designed in Section V assumed a static $\mathbf{H}$ for all symbols, in practice each symbol experiences a unique $\mathbf{H}$ due to the LED non-linearity as discussed in Section IV-C3. Let, $\mathbf{H}(\mathbf{s}_j)$ denote the channel matrix, corresponding to the transmitted symbol $\mathbf{s}_j$. The optimal decoder assumes the receiver has complete channel knowledge (i.e., $\forall j$ $\mathbf{H}(\mathbf{s}_j)$ is known) obtained through a training procedure. The optimal minimum distance decoder is then represented by

$$\mathbf{s}_i^* = \underset{\mathbf{s}_j \in \mathcal{A}}{\arg\min} \quad \|\mathbf{r}_i - \mathbf{H}(\mathbf{s}_j)\mathbf{s}_j\|_2 \tag{16}$$

where $\mathbf{s}_i^*$ is the decoded symbol. The second, sub-optimal, decoder is as in (16), except all symbols are decoded using a fixed $\mathbf{H}$, i.e.,

$$\forall j \; \mathbf{H}(\mathbf{s}_j) = \mathbf{H}_{100}.$$

Fig. 7 depicts the experimental SER versus SNR for the 4, 8 and 16 point constellations presented in Fig. 6, scaled to operate from 0 to 200 mA. Fig. 7(a) depicts the simulated and experimental results for the fixed decoder while Fig. 7(b) depicts the results for the optimal decoder. It is clear from Fig. 7 that the experimental measurements agree with the simulated nonlinear channel in all cases, with minor discrepancies attributed to measurement errors in the SNR and in the decoder training.

Under the fixed decoder, the optimized constellations (Fig. 6 Col. 2) for 4, 8 and 16-CSK outperformed their respective IEEE 802.15.7 standard constellations (Fig. 6 Col. 1) by approximately 1 dB, 3 dB and 1.5 dB in terms of SNR. Under the optimal decoder, the same optimized constellations for 4, 8 and 16-CSK outperformed their respective IEEE 802.15.7 standard constellations by approximately 1, 2 and 1 dB. These results support that assuming a nominal static $\mathbf{H}$ is a reasonable approach to obtain CSK alphabets with better error performance than those currently contained in the IEEE standard. Furthermore, Fig. 7 shows that the SNR penalty for decoding using the simpler fixed decoder ranged from approximately 0 dB (the

TABLE II
OPTIMIZED 3D 8 CSK CONSTELLATIONS

(a) IEEE, $d_{\min}$ = 0.1869

R	0	0	0	0.550	0.061	1.100	0.611	0.384
G	1.100	0	0.384	0.550	0.611	0	0.061	0
B	0	1.100	0.716	0	0.228	0	0.228	0.716

(b) Optimized - Color Unspecified, $d_{\min}$ = 0.3014

R	0	0.069	0.301	0.801	0.381	0	1.100	0.555
G	1.010	0.494	0	0.295	0.575	0	0	0
B	0	0.337	0.799	0	0.091	1.010	0	0.345

(c) Optimized - 3000K, $d_{\min}$ = 0.2227

R	0.463	0.549	0.670	0.885	0.282	0.373	0.772	1.100
G	0	0.395	0	0	0.300	0.659	0.328	0
B	0.436	0	0.230	0.015	0.318	0	0	0

4-CSK constellations), to at worst 4 dB (3000K 16-CSK constellation). Therefore, depending on the constellation, and provided the channel non-linearity is mild, the complexity of the decoder can be reduced.

VII. CONSTRAINT RELAXATION: 3D-CSK

While constant luminous flux and constant current operation have noted advantages, relaxing the constraint to include a set amount of fluctuation, as in (6), can be exploited to improve the minimum distance of CSK constellations. Table II displays the numeric values of 3-D 8-CSK constellations, designed for the channel discussed in Section IV. As in Section V, the total current is constrained instead of luminous flux. Symbols are selected such that $I_{\min} = 0.9$, $I_{\max} = 1.1$, with the peak current constraints inactive, and L unspecified.

As in IEEE 802.15.7, the constellation in Table II(a) was optimized assuming no knowledge of the channel, i.e., an identity channel matrix. The points of Table II(a) have a configuration similar to that of the IEEE standard 8-CSK constellation. The relaxation of the constant sum of all symbol elements produces a constellation with a 0.53 dB improvement in minimum distance over the standard IEEE 8-CSK constellation, after normalizing each constellation to have the same mean L.

Table II(b) is the 3D 8-CSK constellation optimized for $\mathbf{H}_{100}$. Compared to the 2-D 8-CSK constellation (Fig. 6 Col. 2), the constraint relaxation leads to a 0.88 dB improvement in minimum distance.

Lastly, Table II(c) is the 3D 8-CSK constellation derived for the same $\mathbf{d}$ used in the 3000K constellations presented in Fig. 6. Interestingly, not only did the allowable ripple improve the minimum distance by 3.78 dB when compared to its 2-D counterpart (Fig. 6 Col. 3), but the minimum distance of the 3D 3000K 8-CSK constellation is 1.52 dB greater than the constellation in Table II(a). Clearly, relaxing the constant envelope constraint has a greater effect on constellations with a constrained chromaticity near the boundary of the constraint region than those without a chromaticity constraint.

VIII. CONCLUSION

This work presents a comprehensive design framework for CSK constellations based on a deterministic optimization approach. The technique permits designers to constrain luminous flux, current, and color in order to design 2-D and 3-D constellations that are optimized over color channel crosstalk. Consequently, the method was shown to be general enough to be applied to the CIM constellation design problem as well. Furthermore, the design of a prototype CSK channel is presented for the first time. The implemented CSK channel was characterized and constellations were optimized for the measured channel. The SERs versus SNR of each optimized constellation were measured and compared to constellations designed using the current standardized CSK design rules. It was observed that the design methods proposed in this work were able to improve upon the standard constellations with up to a 3 dB gain in SNR. Interesting future directions include augmenting the design constraints to include a color quality metric (e.g., color rendering), as well as non-linear channel compensation.

REFERENCES

[1] Philips. Hue: Personal Wireless Lighting. (2013). [Online]. Available: https://www.meethue.com/

[2] K.-I. Ahn and J. K. Kwon, "Color intensity modulation for multicolored visible light communications," *IEEE Photon. Technol. Lett.*, vol. 24, no. 24, pp. 2254–2257, Dec. 2012.

[3] *IEEE Standard for Local and Metropolitan Area Networks—Part 15.7: Short-Range Wireless Optical Communication Using Visible Light*, IEEE Standard 802.15.7, 2011.

[4] A. Wilkins, J. Veitch, and B. Lehman, "LED lighting flicker and potential health concerns: IEEE standard PAR1789 update," in *Proc. IEEE Energy Convers. Congr. Expo.*, Atlanta, GA, USA, 2010, pp. 171–178.

[5] R. J. Drost and B. M. Sadler, "Constellation design for color-shift keying using billiards algorithms," in *Proc. IEEE GLOBECOM Workshops*, Miami, FL, USA, 2010, pp. 980–984.

[6] B. Bai, Q. He, Z. Xu, and Y. Fan, "The color shift key modulation with non-uniform signaling for visible light communication," in *Proc. 1st IEEE Int. Conf. Commun. China Workshops*, Beijing, China, 2012, pp. 37–42.

[7] P. Butala, J. Chau, and T. D. C. Little, "Metameric modulation for diffuse visible light communications with constant ambient lighting," in *Proc. Int. Workshop Opt. Wireless Commun.*, Pisa, Italy, 2012, pp. 1–3.

[8] E. Monteiro and S. Hranilovic, "Constellation design for color-shift keying using interior point methods," in *Proc. IEEE Globecom Workshops*, Anaheim, CA, USA, 2012, pp. 1224–1228.

[9] Philips Lumileds Lighting Company. (2014). LUXEON Rebel and LUXEON Rebel ES Color Portfolio: Part No. Red: LXM2-PD01-0050, Green: LXML-PM01-0100, Blue: LXML-PB01-0040. [Online]. Available: http://www.luxeonstar.com/v/vspfiles/downloadables/DS68.pdf

[10] J. M. Kahn and J. R. Barry, "Wireless infrared communications," *Proc. IEEE*, vol. 85, no. 2, pp. 265–298, Feb. 1997.

[11] R. Lenk and C. Lenk, *Practical Lighting Design with LEDs*. New York, NY, USA: Wiley, 2011.

[12] Energy Star. Energy Star Program Requirements for Integral LED Lamps. (2011). [Online]. Available: http://www.energystar.gov/ia/partners/product_specs/program_reqs/Integral_LED_Lamps_Program_Requirements.pdf

[13] Y. Ohno, "CIE fundamentals for color measurements," in *Proc. Int. Conf. Digit. Print. Technol.*, Vancouver, BC, Canada, Jan. 2000, pp. 540–545.

[14] R. Gohary and T. Davidson, "Noncoherent MIMO communication: Grassmannian constellations and efficient detection," in *Proc. Int. Symp. Inf. Theory*, Chicago, IL, USA, 2004, p. 65.

[15] *MATLAB Version 7.10.0 (R2010a)*. Natick, MA, USA: The MathWorks Inc., 2010.

[16] Altera. Cyclone II Device Handbook, Volume 1. (2014). [Online]. Available: http://www.altera.com/literature/hb/cyc2/cyc2_cii5v1.pdf

[17] Analog Devices. CMOS, 330 MHz, Triple 10-Bit High Speed Video DAC. (2010). [Online]. Available: http://www.analog.com/static/imported-files/data_sheets/ADV7123.pdf

[18] Linear Technology. LT 1365 Quad 70 MHz, 1000 V/s Op Amp. (2013). [Online]. Available: http://cds.linear.com/docs/en/datasheet/13645fa.pdf

[19] Panasonic Corporation. 2SD2358 Silicon NPN epitaxial planar type. (2003). [Online]. Available: http://www.semicon.panasonic.co.jp/ds4/2SD2358_BED_discon.pdf

[20] Thorlabs Inc. PDA36A Si Switchable Gain Detector. (2011). [Online]. Available: http://www.thorlabs.us/Thorcat/13000/PDA36A-Manual.pdf
[21] LEE Filters. Polyester Filters. Part No. 024 (Scarlet), 738 (Jas Green), 079 (Just Blue). (2013). [Online]. Available: http://www.leefilters.com/lighting/colour-details.html
[22] Agilent Technologies. Infiniium 54850 Series Oscilloscopes and InfiniiMax 1130 Series Probes Data Sheets. (2005). [Online]. Available: http://cp.literature.agilent.com/litweb/pdf/5988-7976EN.pdf
[23] E. Monteiro, "Design and implementation of color-shift keying for visible light communications," Master's thesis, Dept. Elect. Comput. Eng., McMaster Univ., Hamilton, ON, Canada, 2013.

Eric Monteiro (S'08–M'13) received the Bachelor Engineering and Management degree in electrical engineering from McMaster University, Hamilton, ON, Canada in 2011, where he then joined the Free Space Optical Algorithms Laboratory and received the M.A.Sc. degree in 2013. His research interests include area of optimization, communication systems, and high-speed circuit design.

Steve Hranilovic (S'94–M'03–SM'07) received the B.A.Sc. (Hons.) degree in electrical engineering from the University of Waterloo, Waterloo, ON, Canada, in 1997, and the M.A.Sc. and Ph.D. degrees in electrical engineering from the University of Toronto, Toronto, ON, in 1999 and 2003, respectively. He is currently an Associate Professor in the Department of Electrical and Computer Engineering, McMaster University, Hamilton, ON, where he also serves as the Associate Chair for Undergraduate Studies. During 2010-2011, he spent his research leave as a Senior Member, Technical Staff in advanced technology for Research in Motion, Waterloo. His research interests include the areas of free-space and optical wireless communications, digital communication algorithms, and electronic and photonic implementation of coding and communication algorithms. He is the author of the book *Wireless Optical Communication Systems* (New York, NY, USA: Springer, 2004). Dr. Hranilovic is a licensed Professional Engineer in the Province of Ontario and received the Government of Ontario Early Researcher Award in 2006. He currently serves as an Editor for the IEEE TRANSACTIONS ON COMMUNICATIONS in the area of optical wireless communications.